Properties of Selected High-Strength Composite Conductors With Different Strengthening Components

Ke Han, Jun Lu, Vince Toplosky, Rongmei Niu, Robert Goddard, Yan Xin, Robert Walsh, Iain Dixon, and Victor Pantsyrny

***Abstract*—High field magnets require the development and fabrication of large quantities of conductors with both high strength and high electrical conductivity. This combination of properties can be obtained from copper matrix composites either in macroscopic or microscopic form. Deformation can strengthen these composites further by either inducing dislocations or refining microstructure. During deformation, the strengthening component either retains its original shape or flows with the matrix, depending on its original hardness. In general, a non-deformable component is initially harder than one that deforms with the matrix. Co-deformation in both component and matrix leads to very high strength levels that are significantly greater than those that can be achieved in composites strengthened by non-deformable components. Thus, to properly choose a system for application in high field magnets, we must consider the detailed mechanisms of strengthening that are operative in materials with ultra-fine scale microstructure. In this paper, we compare composites strengthened by either deformable or non-deformable components and describe parameters for the design and fabrication of materials selected for high field magnets.**

***Index Terms*—High strength conductors, copper, deformation, high field magnet, conductivity.**

I. Introduction

HIGH field magnets require high-strength and high electrical conductivity coils. The coils need the conducting wire, a reinforcement system, and an insulating material. An overview of the materials requirements for a variety of magnet systems including pulse magnets, quasicontinuous magnets, resistive DC magnets and hybrid magnets is given in the recent comprehensive text and also in various volumes of the IEEE transactions on magnetics since 1990 [1]–[4]. In the current paper, consideration is given only to the development of the conductors required for high field magnets. The major portion of the paper will be devoted to comparison of high-strength composite conductors. In those conductors, the codeformation behavior of matrix and the strengthening component will be discussed in details.

High-strength conductors can be manufactured from ceramic particle strengthened composites, where strengthening component won't be deformed with the Cu matrix [5]–[8]. These conductors can also be made from macroscopic systems such as cold deformed copper and structure materials and the deformation of a variety of in situ composites [9]. The essential relations to be established are between the design needs of the magnet system, the structure and properties of the conductor, and the methods of fabrication required to produce conductor systems of the required dimensions. These aspects will be discussed in separate sections of this paper.

The strength levels required in the high strength conductors are of the order of 0.5 to 1.5 GPa, which is of the order of one thirtieth of the shear modulus for copper bases alloys. Hence the materials have strength levels within a factor of two or three of the theoretical strength due to the extremely fine structures developed by wire drawing. Thus it is appropriate to include in this paper some consideration of the features which determine both the strength and conductivity in these materials together with a brief discussion of future areas of fruitful research.

II. Methods

A. Materials

Most of precursors referred in this paper were made by collaborators of the National High Magnetic Field Laboratory (MagLab). Cold deformation and heat treatment were undertaken in MabLab.

B. Testing Methods

Most mechanical tests were performed at 295 K and 77 K on a 100 kN servo-hydraulic MTS test machine. In tensile tests, the samples were loaded at a displacement control rate

Manuscript received September 24, 2019; accepted March 9, 2020. Date of publication March 18, 2020; date of current version April 17, 2020. This work was undertaken in the National High Magnetic Field Laboratory, which is supported by US National Science Foundation through DMR-1157490 plus DMR-1644779 and the State of Florida. The microscopes were funded by Florida State University Research Foundation and Florida State. *(Corresponding author: Ke Han.)*

Ke Han, Jun Lu, Vince Toplosky, Rongmei Niu, Robert Goddard, Yan Xin, Robert Walsh, and Iain Dixon are with the National High Magnetic Field Laboratory, Tallahassee, FL 32309 USA (e-mail: han@magnet.fsu.edu; junlu@magnet.fsu.edu; toplosky@magnet.fsu.edu; rniu@magnet.fsu.edu; goddard@magnet.fsu.edu; xin@magnet.fsu.edu; walsh@magnet.fsu.edu; idixon@magnet.fsu.edu).

Victor Pantsyrny is with the Nanoelectro, LLC, Moscow 123098, Russia (e-mail: pantsyrny@gmail.com).

Color versions of one or more of the figures in this article are available online at https://ieeexplore.ieee.org.

Digital Object Identifier 10.1109/TASC.2020.2981270

of 0.5 mm/min. An unload/reload cycle was performed to determine the elastic modulus. Extensometers with gage length between 10 and 25 mm were used to record strain, and a 100 kN load cell to measure force. From the measured stress-strain curves, both ultimate tensile strength (UTS) and 0.2% offset engineering flow stress (YS) were recorded.

The resistivity measurements were performed on full cross-sectional samples. Voltage taps were mechanically clamped on the specimens at approximately 100 mm apart. Current leads were attached to the ends of the specimens. After room temperature testing, the samples and fixture were completely submerged in a liquid nitrogen filled dewar. RRR is the value of resistivity at room temperature over resistivity at 77 K. In total, six samples were tested and the value reported is the average of the measurements and is estimated to be accurate within +/−1% IACS.

C. Microstructure Examinations

Microstructure was investigated by a Zeiss 1540XB and a FEI Helios G4 UC field emission gun scanning electron microscopes (FEG SEM), Energy Dispersion X-ray (EDX) spectrometers were attached to both SEMs. Transmission electron microscopy (TEM) observations were carried out using a JEOL 002 ARM operating at 200 kV [10], [11].

III. Results

A. Composite Conductors Before Cold Work

The fabrication of conductors starts, in most cases, with one of three processes: solidification, consolidation, or sintering. In solidified composites, the strengthening component is usually created during both solidification and subsequent heat treatment. In consolidated composites, the strengthening component usually maintains its predesigned size and shape. Different fabrication methods lead to different distribution patterns, density levels, and particle shapes, each influencing strength levels to a greater or lesser degree.

In our laboratory, one of the precursors used is GlidCop, which is a group of copper-matrix conductors (Al15, Al25 and Al60) strengthened by alumina particles. These conductors have relatively high strength in as-consolidated conditions. Al15, for example has an ultimate tensile strength level of 393 MPa and 0.2% offset flow strength of 324 MPa without any cold work. Al 60 has even higher tensile strength (Fig. 1). Both of these strength levels are much higher than can be achieved in most other Cu matrix conductors that have not subjected to cold work.

Because of the coarse microstructure of Cu–Nb in as-cast condition [12]–[15], Cu–Nb composite ingots usually have lower mechanical strength than Cu-alumina billets. Cu–Nb composite, however, has much higher ductility and work-hardening rate (Fig. 1). Therefore, if large deformation strain can be used, it can achieve significantly higher mechanical strength than Cu-alumina.

Because of the coarse microstructure of Cu–Ag in as-cast condition, Cu–Ag ingots also have lower mechanical strength

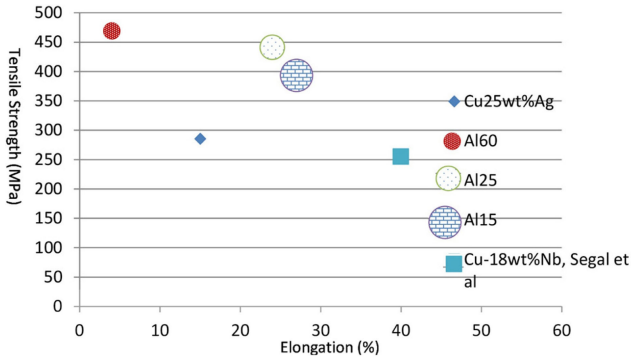

Fig. 1. Comparison of ultimate tensile strength levels of composite conductors with deformable strengthening component and un-deformable strengthening component. Al15, Al25, and Al60 are conductors with alumina un-deformable particles and denoted by large round solid circles. Their work-hardening rates are relatively low. Cu–Ag is strengthened by deformable fibers and denoted by small solid diamond, indicating that relatively small ingot is required in order to achieve high strength. Cu–Nb is strengthened by deformable ribbons and denoted by medium sized solid squire, indicating medium sized ingot is needed to achieve high strength.

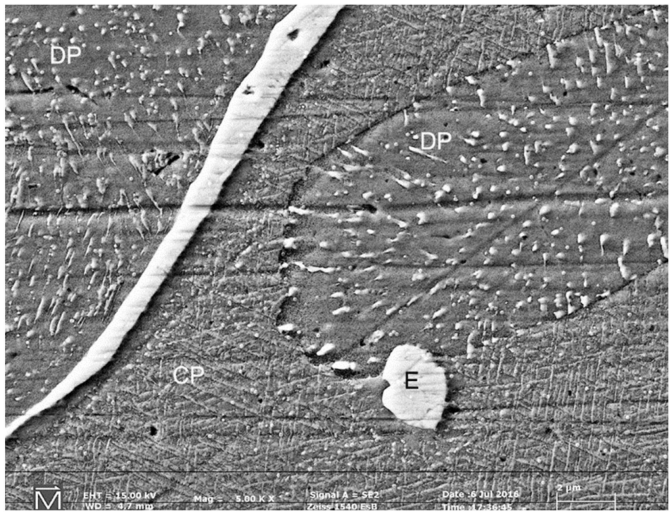

Fig. 2. Scanning electron microscopy image showing eutectic component (indicated by E) and proeutectic component. Both continuous precipitates (denoted by CP) and discontinuous precipitates (denoted by DP) occur in proeutectic component. The spacing between DP is about a few micrometers. The microbar is 2 μm in the image.

than Cu-alumina billets (Fig. 1). In this case, however, Ag particles can sometimes precipitate out from the supersaturated solid solution formed during casting, giving Cu–Ag ingots higher mechanical strength than Cu–Nb ingots (Fig. 2) [16]–[19].

Cu–Ag composites have a higher work-hardening rate than Cu-alumina, as well as sufficient ductility for deformation. They have been found to achieve higher strength than Cu-alumina, but not as high as Cu–Nb.

We have observed both continuous and discontinuous precipitates in Cu–Ag ingots. Using DSC in combination with microstructure examination, we found that higher temperatures with higher activation energies were often associated with a great number of continuous precipitates (CPs) throughout the

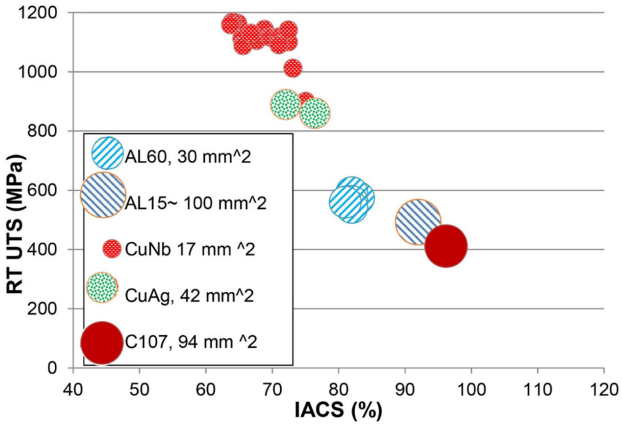

Fig. 3. Comparison of room temperature (RT) tensile strength (MPa) and RT conductivity 100%IACS (International Annealed Copper Standard, 100%IACS is equivalent to 1.724 $\mu\Omega$cm) of selected conductors in wire form; Al15, and Al60 are conductors with alumina un-deformable particles and denoted by large round circles, C107 is Cu+0.085wt%Ag and is denoted by a large solid circle. Cu–Ag, which has Ag content between 24-25wt%, is strengthened by Ag fibers. Cu–Nb is strengthened by deformable ribbons and denoted by small sized solid circles, indicating small cross-section conductors. All composite conductors are in cold deformed condition.

Cu matrix. Lower temperatures with lower activation energies, however, were associated with a predominance of coarse discontinuous precipitates (DPs), largely concentrated around grain boundaries. CPs, because they are usually finer and occur in greater density, tend to have a greater strengthening effect.

In ingots of as-cast condition, spacing between CP is as fine as 0.1 μm, leading to relatively high strengthening effects. Spacing between DP, on the other hand, is in micrometer scale (Fig. 2). By doping the composite with other alloying elements, we were able to achieve the effect of altering activation energies and precipitation temperatures. This leads to changes in the density and volume fraction of continuous precipitates in the doped composite. An increased volume fraction of continuous precipitates results in higher mechanical strength. The strength level, however, is still below the requirement of most high field magnets. Cold-deformation is required to enhance the mechanical strength further.

B. Composite Conductors After Cold Work

High-field pulsed and DC-resistive magnets rely on copper alloys that combine high strength and high electrical conductivity (HSHC). Researchers have been developing better HSHC materials for many decades. In US MagLab, most pulsed magnets depend on four different HSHC materials. Conductors for these magnets must have not only high strength and high conductivity but also the capability of being fabricated in appropriate sizes. Cu alloys doped with other alloying elements, such as 0.085wt%Ag have been fabricated into wire with very large cross-section area (see Fig. 3). In this paper, Cu alloys doped with less than 0.5wt% Ag are distinguished from other Cu–Ag composites by the abbreviation Cu(Ag). These Cu(Ag) conductors are usually commercially available and can be made into very long wire with very large cross-section area. Our tests indicated that this type of conductor has electrical conductivity greater than 95% IACS. Because of low alloy content, however, the strain hardening rate is usually low in this material, yielding a maximum achievable strength up to only about 0.5 GPa. At this stress level, the average ratio of ultimate tensile strength (UTS) over yield strength (YS) is below 1.05 ± 0.03, indicating that, because of dynamic recovery and recrystallization, the composite has little room for further work-hardening.

Al15 billets, which are commercially available, can reach higher mechanical strength than Cu(Ag). Our results indicated that Al15 wires with cross-section close to 100 mm^2 could reach mechanical strength greater than 0.47 GPa after cold deformation. At this stress level, however, the average ratio of UTS over YS was below 1.06 ± 0.03, a little higher than Cu(Ag), but still leaving little room for further work-hardening.

Al60 billets reached much higher mechanical strength than Al15 after cold deformation. These billets are commercially available with copper cladding. Our results indicated that Al60 Cu-clad wire with cross-section close to 30 mm^2 can reach mechanical strength greater than 0.56 GPa after cold deformation. Without copper cladding, however, the mechanical strength reached above 0.6 GPa in some cases, especially when deformation strain was greater than 75%. At this stress level, the average ratio of UTS over YS was up to 1.09 ± 0.04, slightly higher than for Al15. Al60 might be expected to have more room than Al15 for further work-hardening, but this does not occur because larger alumina particles (found using our TEM) cause the wire to fracture before hardening.

We found that the conductivity values for Cu(Ag) and GlidCop were both between 80 to 95% IACS. Even though alumina is less soluble than Ag in Cu matrix, we found that, contrary to our expectation, the conductivity of Cu(Ag) actually exceeded that of alumina-strengthened Cu (Fig. 3).

We found that in our Cu–Ag composites with Ag content higher than 5wt%, strength greater than 900 MPa was achievable. This type of composite, however, is not commercially available. After cold deformation, our Cu–Ag conductors reached higher mechanical strength than either Al60 or Cu(Ag). The maximum true strain for achieving high strength in our Cu–Ag conductors was only 4.8. Thus we were able to fabricate wire with cross-section area greater than 40 mm^2 from relatively small ingots (diameter $\sim$0.1 meter). The conductivity of these wires was around 70% IACS (lower than either Cu(Ag) or Al60) because of their higher Ag content and refined microstructure.

After cold deformation, Cu–Nb reached higher mechanical strength than any of other conductors that we tested. Our data showed that Cu–Nb wire with cross-section area $\sim$17 mm^2 can reach mechanical strength greater than 1 GPa after cold deformation [20]–[34]. This material, however, is not commercially available in either ingots or billets. In order to reach high strength, our wires were subjected to high deformation strain, i.e., true strain greater than 10. To obtain such great deformation strain values, we had to work with Cu–Nb that

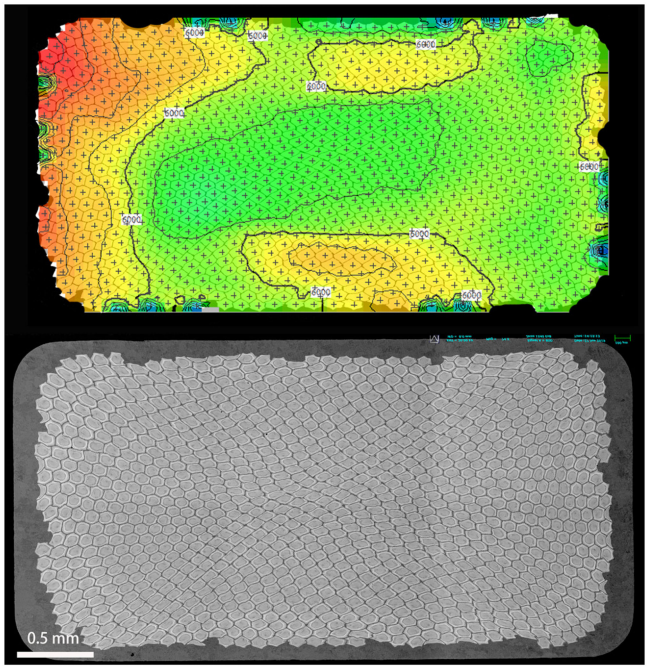

Fig. 4. Cross-section SEM image (image at the bottom) and area mapping (image at the top) of a Cu–Nb conductor. Between sub-elements (grey areas in SEM image) area copper claddings (dark lines). Copper cladding is also surrounded the sub-elements. The cross-section area is different in different locations (top image). At left side, the cross-section area of individual elements is larger than the ones on right.

had been cladded and restacked. Restacking created bundles (sub-elements) of nano-sized deformable ribbons. Because of incompatibility between fcc-Cu and bcc-Nb, heavy deformation may generate inhomogeneous strain in different sub-elements, leading to differences in ribbon spacing at macro-scale (Fig. 4). This may lead to differences in mechanical properties in different areas within a single conductor wire.

After removal of copper cladding, mechanical strength reached above 1.1 GPa in heavily deformed Cu–Nb, and the average ratio of UTS over YS remained higher than most of the conductors we tested (1.4 ± 0.1). Consequently, Cu–Nb composite has the potential to be work-hardened further to reach even higher mechanical strength. Because of the high strength level, however, conductivity was below 70% IACS.

C. Cryogenic Properties

The cryogenic property data reported here were all obtained from materials after deformation because pulsed magnets, which are usually made from cold-deformed conductors, are generally operated at cryogenic temperatures. All the conductors we tested showed higher mechanical strength at 77 K than at room temperature. Dynamic recovery and recrystallization were suppressed at 77 K, leading to higher mechanical strength.

RRR values for pure Cu are usually high, even in as-deformed conditions [35]. RRR in Cu–Ag conductors was only ~ 3, lowest among all the conductors studied in this work [36]–[40]. The reason is that the presence of dissolved alloying elements, of which Ag is one, reduces RRR values. RRR was higher in Cu–Nb than in Cu–Ag because the Cu cladding in Cu–Nb remained pure and Nb was less soluble than Ag in Cu matrix. Both Cu–Ag and Cu–Nb contained deformable strengthening components. This may be the reason why deformation reduced the conductivity and the RRR of both materials. The RRR values of both Al15 and Cu(Ag) were higher than 4 because of low content of alloying elements. GlidCop conductors contained a non-deformable strengthening component, so cold deformation had limited impact on either their conductivity or their RRR values.

IV. Discussion

A. Mechanical Strength

To achieve highest mechanical strength, the spacing between the strengthen component has to be reduced to below 100 nm. Such a fine scale is difficult to achieve in materials in either as-consolidated condition or as-cast conditions. Severe plastic deformation is therefore required. To achieve such a goal, the materials need to have high ductility and high work-hardening rate.

B. Electrical Conductivity

Even without introducing dissolvable alloying elements, refinement of microstructure can induce some dissolution of strengthening component, particularly when the strengthening component is deformable. Therefore, for a certain applications, an optimized microstructure should be designed in order to achieve optimized combination of mechanical strength and electrical conductivity.

V. Conclusions

Conductors strengthened by non-deformable components reached strength levels greater than 0.4 GPa in as-consolidated form. Cold deformation had almost no impact on their conductivity. Consequently, these conductors could be used for pulsed magnets after a relatively small amount of cold-deformation. As-cast conductors strengthened by deformable components had lower strength levels than those strengthened by non-deformable components. Those with deformable strengthening components, however, reached higher strength in as-deformed conditions when deformation strain was also very high. Deformation reduced electrical conductivity more in conductors with deformable components than in those with non-deformable components. In both types, mechanical strength and electrical conductivity values were dependent on the volume fraction of the strengthening component.

Acknowledgment

We thank Drs. Nguyen and Bird for discussions, NAH, Nanoelectro, ACI Alloys for supplying composites, Sam Dong for wire drawing, and Dr. Tyler for editing the manuscript. This work was undertaken in the National High Magnetic Field Laboratory.

REFERENCES

[1] J. L. Bacon *et al.*, "The US NHMFL 100 tesla multi-shot magnet," *IEEE Trans. Appl. Supercond.*, vol. 12, no. 1, pp. 695–698, Mar. 2002.

[2] H. J. Schneider-Muntau, K. Han, N. A. Bednar, C. A. Swenson, and R. Walsh, "Materials for 100 T monocoil magnets," *IEEE Trans. Appl. Supercond.*, vol. 14, no. 2, pp. 1153–1156, Jun. 2004.

[3] C. A. Swenson *et al.*, "Performance of 75 T prototype pulsed magnet," *IEEE Trans. Appl. Supercond.*, vol. 16, no. 2, pp. 1650–1655, Jun. 2006.

[4] C. A. Swenson *et al.*, "Progress of the insert coil for the US-NHMFL 100T multi-shot pulse magnet," *Physica B-Condensed Matter*, vol. 346, pp. 561–565, 2004.

[5] K. Han, R. E. Goddard, V. J. Toplosky, R. Niu, J. Lu, and R. Walsh, "Alumina particle reinforced Cu matrix conductors," *IEEE Trans. Appl. Supercond.*, vol. 28, no. 3, Apr. 2018, Art. no. 7000305.

[6] J. F. Jin, W. L. Xiao, and H. B. Chen, "Thermal fatigue life of glidcop Al-15 high-heat-load components," in *Iscm Ii and Epmesc Xii, Pts 1 and 2*, J. W. Z. Lu, A. Y. T. Leung, V. P. Iu, and K. M. Mok, Eds., Hong Kong: Amer. Inst. Phys., 2010, pp. 982–986.

[7] T. J. Miller, S. J. Zinkle, and B. A. Chin, "Strength and gatigue of dispersion-strengthened copper," *J. Nucl. Mater.*, vol. 179, pp. 263–266, 1991.

[8] J. D. Troxell, A. V. Nadkarni, and R. R. Solomon, "Properties and performance of GlidCop (R) DSC in temperature range of 20-350 degrees C," in *Proc. Process. Fabr. Adv. Mater.*, 1996, pp. 755–774.

[9] J. D. Embury and K. Han, "Dislocation accumulation at large plastic strains - An approach to the theoretical strength of materials.," *Progress Mech. Behaviour Mater. (Icm8)*, vol. 2, pp. 448–457352, 1999.

[10] Y. Xin, K. Han, Z. Liang, Y.-F. Su, P. J. Lee, and D. C. Larbalestier, "Aberration-corrected S/TEM at Florida State University," *Microsc. Today*, vol. 22, no. 3, pp. 42–49, 2014.

[11] Y. Xin *et al.*, "Facility implementation and comparative performance evaluation of probe-corrected TEM/STEM with schottky and cold field emission illumination," *Microsc. Microanalysis*, vol. 19, no. 2, pp. 487–495, 2013.

[12] W. A. Spitzig, "Strengthening in heavily deformation processed Cu-20-percent Nb," *Acta Metallurgica Et Materialia*, vol. 39, no. 6, pp. 1085–1090, 1991.

[13] W. A. Spitzig, L. S. Chumbley, J. D. Verhoeven, Y. S. Go, and H. L. Downing, "Effect of temperature on the strength and conductivity of a deformation processed Cu-20-percent-Fe composite," *J. Mater. Sci.*, vol. 27, no. 8, pp. 2005–2011, 1992.

[14] W. A. Spitzig, H. L. Downing, F. C. Laabs, E. D. Gibson, and J. D. Verhoeven, "Strength and electrical-conductivity of a deformation-processed Cu-5 PCT Nb composite," *Metallurgical Trans. a-Physical Metall. Mater. Sci.*, vol. 24, no. 1, pp. 7–14, 1993.

[15] W. A. Spitzig, S. T. Kim, and P. M. Berge, "Development of low concentration deformation processed Cu–Nb and Cu–Cr alloys," *Mater. Manuf. Processes*, vol. 10, no. 3, pp. 353–371, 1995.

[16] C. A. Davy, K. Han, P. N. Kalu, and S. T. Bole, "Examinations of Cu–Ag composite conductors in sheet forms," *IEEE Trans. Appl. Supercond.*, vol. 18, no. 2, pp. 560–563, Jun. 2008.

[17] K. Han, J. D. Embury, J. J. Petrovic, and G. C. Weatherly, "Microstructural aspects of Cu–Ag produced by the Taylor wire method," *Acta Materialia*, vol. 46, no. 13, pp. 4691–4699, Aug 1998.

[18] K. Han, R. Niu, J. Lu, and V. Toplosky, "High strength conductors and structural materials for high field magnets," *MRS Advances*, vol. 1, no. 17, pp. 1233–1239, 2016.

[19] G. M. Li, Y. Liu, Y. Su, E. G. Wang, and K. Han, "Influence of high magnetic field on as-cast structure of Cu-25wt%Ag alloys," *China Foundry*, vol. 10, no. 3, pp. 162–166, 2013.

[20] B. Z. Cui, Y. Xin, and K. Han, "Structure and transport properties of nanolaminate Cu–Nb composite foils by a simple fabrication route," *Scripta Materialia*, vol. 56, no. 10, pp. 879–882, 2007.

[21] L. Deng *et al.*, "Response of microstructure to annealing in in situ Cu–Nb microcomposite," *J. Mater. Sci.*, vol. 54, no. 1, pp. 840–850, 2019.

[22] L. P. Deng *et al.*, "Hardness, electrical resistivity, and modeling of in situ Cu–Nb microcomposites," *J. Alloys Compounds*, vol. 602, pp. 331–338, 2014.

[23] L. P. Deng, K. Han, B. S. Wang, X. F. Yang, and Q. Liu, "Thermal stability of Cu–Nb microcomposite wires," *Acta Materialia*, vol. 101, pp. 181–188, 2015.

[24] L. P. Deng, K. Han, B. S. Wang, X. F. Yang, and Q. Liu, "Thermal stability of Cu–Nb microcomposite wires (vol 101, pg 181, 2015)," *Acta Materialia*, vol. 105, pp. 519–519, 2016.

[25] L. P. Deng, K. Han, X. F. Yang, Z. Y. Sun, and Q. Liu, "Effect of extra Cu on the strength and conductivity of Cu–Nb microcomposite wires," *Rare Metal Mater. Eng.*, vol. 44, no. 7, pp. 1696–1701, 2015.

[26] L. P. Deng, B. S. Wang, H. L. Xiang, X. F. Yang, R. M. Niu, and K. Han, "Effect of annealing on the microstructure and properties of In-situ Cu–Nb microcomposite wires," *Acta Metall. Sin.-Engl. Lett.*, vol. 29, no. 7, pp. 668–673, 2016.

[27] L. P. Deng, X. F. Yang, K. Han, Y. F. Lu, M. Liang, and Q. Liu, "Microstructure and texture evolution of Cu–Nb composite wires," *Mater. Characterization*, vol. 81, pp. 124–133, 2013.

[28] L. P. Deng, X. F. Yang, K. Han, Z. Y. Sun, and Q. Liu, "Study on the microstructure evolution of Cu–Nb composite wires during deformation and annealing," *Acta Metallurgica Sinica*, vol. 50, no. 2, pp. 231–237, 2014.

[29] K. Han *et al.*, "Material issues in the 100 T non-destructive magnet," *IEEE Trans. Appl. Supercond.*, vol. 10, no. 1, pp. 1277–1280, Mar. 2000.

[30] K. Han *et al.*, "The fabrication, properties and microstructure of Cu–Ag and Cu–Nb composite conductors," *Mater. Sci. Eng. a-Structural Mater. Properties Microstructure Process.*, vol. 267, no. 1, pp. 99–114, 1999.

[31] K. Han *et al.*, "Bending behavior of high-strength conductor," *IEEE Trans. Appl. Supercond.*, vol. 26, no. 4, 2016, Art. no. 8400804.

[32] K. Han, A. Ishmaku, Y. Xin, and P. N. Kalu, "Cold-deformed Cu–Ag and Cu–Nb composites," in *Proc. TMS Annu. Meet. Ultrafine Grained Materials III*, Orlando, FL, USA, 2003, pp. 273–278.

[33] K. Han, V. J. Toplosky, R. Walsh, C. Swenson, B. Lesch, and V. I. Pantsyrnyi, "Properties of high strength Cu–Nb conductor for pulsed magnet applications," *IEEE Trans. Appl. Supercond.*, vol. 12, no. 1, pp. 1176–1180, Mar. 2002.

[34] A. Ishmaku and K. Han, "Characterization of cold-rolled Cu–Nb composite," *Materials Sci. Forum*, vol. 453, pp. 479–484, 2004.

[35] K. Han, R. P. Walsh, A. Ishmaku, V. Toplosky, L. Brandao, and J. D. Embury, "High strength and high electrical conductivity bulk Cu," *Philos. Mag.*, vol. 84, no. 34, pp. 3705–3716, 2004.

[36] C. C. Zhao, X. W. Zuo, E. G. Wang, and K. Han, "Strength of Cu-28 wt%Ag composite solidified under high magnetic field followed by cold drawing," *Metals Mater. Int.*, vol. 23, no. 2, pp. 369–377, 2017.

[37] C. C. Zhao, X. W. Zuo, E. G. Wang, R. M. Niu, and K. Han, "Simultaneously increasing strength and electrical conductivity in nanostructured Cu–Ag composite," *Mater. Sci. Eng. a-Structural Mater. Properties Microstructure Process.*, vol. 652, pp. 296–304, 2016.

[38] X. W. Zuo, R. Guo, C. C. Zhao, L. Zhang, E. G. Wang, and K. Han, "Microstructure and properties of Cu-6wt% Ag composite thermomechanical-processed after directionally solidifying with magnetic field," *J. Alloys Compounds*, vol. 676, pp. 46–53, 2016.

[39] X. W. Zuo, K. Han, C. C. Zhao, R. M. Niu, and E. G. Wang, "Microstructure and properties of nanostructured Cu28 wt%Ag microcomposite deformed after solidifying under a high magnetic field," *Mater. Sci. Eng. a-Structural Mater. Properties Microstructure Process.*, vol. 619, pp. 319–327, 2014.

[40] X. W. Zuo, K. Han, C. C. Zhao, R. M. Niu, and E. G. Wang, "Precipitation and dissolution of Ag in ageing hypoeutectic alloys," *J. Alloys Compounds*, vol. 622, pp. 69–72, 2015.